

Chapter 19

Mascarene High, Australian High, and Antarctic Oscillation Simulated by FGOALS-s2

Dan Sun, Tianjun Zhou and Feng Xue

Abstract The performance of the flexible global ocean-atmosphere-land system model, spectral version 2 (FGOALS-s2) developed by the institute of Atmospheric Physics/State Key Laboratory of numerical modeling for atmospheric sciences and geophysical fluid dynamics (IAP/LASG) is assessed by analyzing the simulation of the present-day climate in the Southern Hemisphere. Future changes in the Southern Hemispheric climate are projected for four representation concentration pathways (RCPs). The major features of climate mean states in the Southern Hemisphere, including the reverse sea level pressure (SLP) anomaly distribution between subtropical and high latitudes, are effectively simulated. Under four RCPs scenarios, the intensity of the Mascarene High (MH) will weaken at the start of the twenty first century and will be enhanced in the beginning of the 2030s; the opposite is predicted for the Australian High (AH). The future evolution of Antarctic Oscillation (AAO) is scenario dependent but clearly tends to intensify under RCP6.0 and RCP8.5 scenarios.

Keywords Southern hemisphere atmospheric circulation · Mascarene high · Australian high · Antarctic oscillation

D. Sun (✉) · T. Zhou · F. Xue
State Key Laboratory of Numerical Modeling for Atmospheric Sciences
and Geophysical Fluid Dynamics (LASG), Institute of Atmospheric Physics,
Chinese Academy of Sciences, Beijing 100029, China
e-mail: sundan@lasg.iap.ac.cn

F. Xue
International Center for Climate and Environment Sciences (ICCES), Institute of
Atmospheric Physics, Chinese Academy of Sciences, Beijing 100029, China

D. Sun
Beijing Meteorological Bureau, Beijing 100089, China

19.1 Introduction

Land–sea distribution and orographic features result in salient differences in atmosphere circulations in the Northern and Southern Hemispheres. However, in the climate research community, less attention has been devoted to the Southern Hemisphere circulation than the Northern Hemisphere circulation.

Both the Mascarene High (MH) and the Australian High (AH) are prominent circulation systems occurring in the Southern Hemisphere and are part of the Asian–Australian monsoon system. Observational analyses have reported significant influences of MH and AH on the boreal summer rainfall in eastern China (Xue et al. 2003; Xue and He 2005). Antarctic Oscillation (AAO), or the Southern Annular Mode, is an additional dominant mode of the Southern Hemisphere that significantly influences the East Asian climate (Gong and Wang 1999; Nan and Li 2003). Data analysis has indicated that the AAO and the related MH and AH activities in boreal spring provide useful information for prediction of the East Asian summer monsoon (Xue et al. 2004). Therefore, understanding and predicting the circulation anomalies in the Southern Hemisphere are of great importance to residents of East Asia.

Southern Hemisphere circulations including the AAO are useful metrics for gauging model performance (Zhou and Yu 2004). Projected scenarios of future climate change indicate an enhanced trend of AAO (Miller et al. 2006). The previous version of the flexible global ocean-atmosphere-land system model (FGOALS) showed moderate skill in the simulation of AAO (Zhou et al. 2005a, b). However, reliability of the updated FGOALS model for the Southern Hemisphere remains unknown. A recent study by Zhou et al. (2013a) has provided a preliminary evaluation on the performance of FGOALS-s2 in this regard. Major results of the simulation and projection of MH, AH, and AAO are outlined and further discussed in the present short note.

19.2 Model and Data

The coupled model used in this study was the FGOALS-s2, which employs as its atmospheric component a new version of the spectral atmospheric model (SAMIL2.0) developed by the institute of Atmospheric Physics/State Key laboratory of numerical modeling for atmospheric sciences and geophysical fluid dynamics (LASG/IAP; Bao et al. 2013). The model data was obtained from CMIP5 experiments, including the twentieth century historical climate simulation and the twenty first century climate change projection, which consists of four representation concentration pathways (RCPs) scenarios with various parameters such as greenhouse gas and aerosol concentrations (Moss et al. 2008).

Additional datasets used in this study include the national centers for atmospheric prediction/national center for atmospheric research (NCEP/NCAR)

reanalysis data, which is available on a $2.5^\circ \times 2.5^\circ$ grid (Kalnay et al. 1996), and twentieth century reanalysis (20CR) data, which is available on a $1^\circ \times 1^\circ$ grid (Compo et al. 2011). For ease of model data comparison, all data were interpolated to a common $2.5^\circ \times 2.5^\circ$ grid by using a bilinear interpolation method. To facilitate discussion, all reanalysis data are referred as “observation” in the following section.

Three indices were used in this study. The MH index and AH index are defined as the mean sea level pressure (SLP) in the range of (25–35°S, 40–90°E) and (25–35°S, 120–150°E), respectively (Xue et al. 2004). To reduce the impact of model bias in mean state simulation, the zonal average was removed (Zhou et al. 2009). The AAO index is defined as the deviation between the normalized zonal mean SLP of 40°S and 65°S (Gong and Wang 1999).

In addition, periods of December–January–February (DJF) and June–July–August (JJA) are defined as boreal winter and summer, i.e., austral summer and winter, respectively.

19.3 Results

19.3.1 *The Climatological Mean States in the Southern Hemisphere*

The 1979–2005 mean JJA and DJF SLP derived from observations and simulations are shown in Fig. 19.1. The observed SLP is featured by a subtropical high-pressure belt and a circumpolar low-pressure zone in both seasons, with three high-pressure centers in the southern oceans, respectively (Fig. 19.1a, b). These features were effectively reproduced in FGOALS-s2 simulation, although the simulated SLP was lower (higher) than the observation South (North) of 45°S in JJA. During DJF, the simulation was lower than the observation between 45 and 60°S but was higher in other regions. The pattern correlation coefficients between observation and simulation were 0.62 for JJA and 0.91 for DJF, both statistically significant at the 5 % level.

The 1979–2005 mean JJA and DJF wind fields at 850 hPa and zonal wind at 200 hPa from the observations and the simulations are shown in Fig. 19.2. In the observation, prominent anti-cyclones appeared over the subtropical oceans and Australia; the southern ocean south to 60°S was dominated by westerlies (Fig. 19.2a, b). The observed circulation features were reasonably simulated by FGOALS-s2 except that the westerly south to 30°S was stronger than the observation in JJA. The bias in DJF differed from that in JJA; the westerly between 30 and 50°S was stronger than the observation, and that south of 50°S was weaker than the observation (Fig. 19.2e, f). Although the centers of the three subtropical high pressures over the southern oceans were reasonably simulated in DJF, the results of JJA were stronger than the observations.

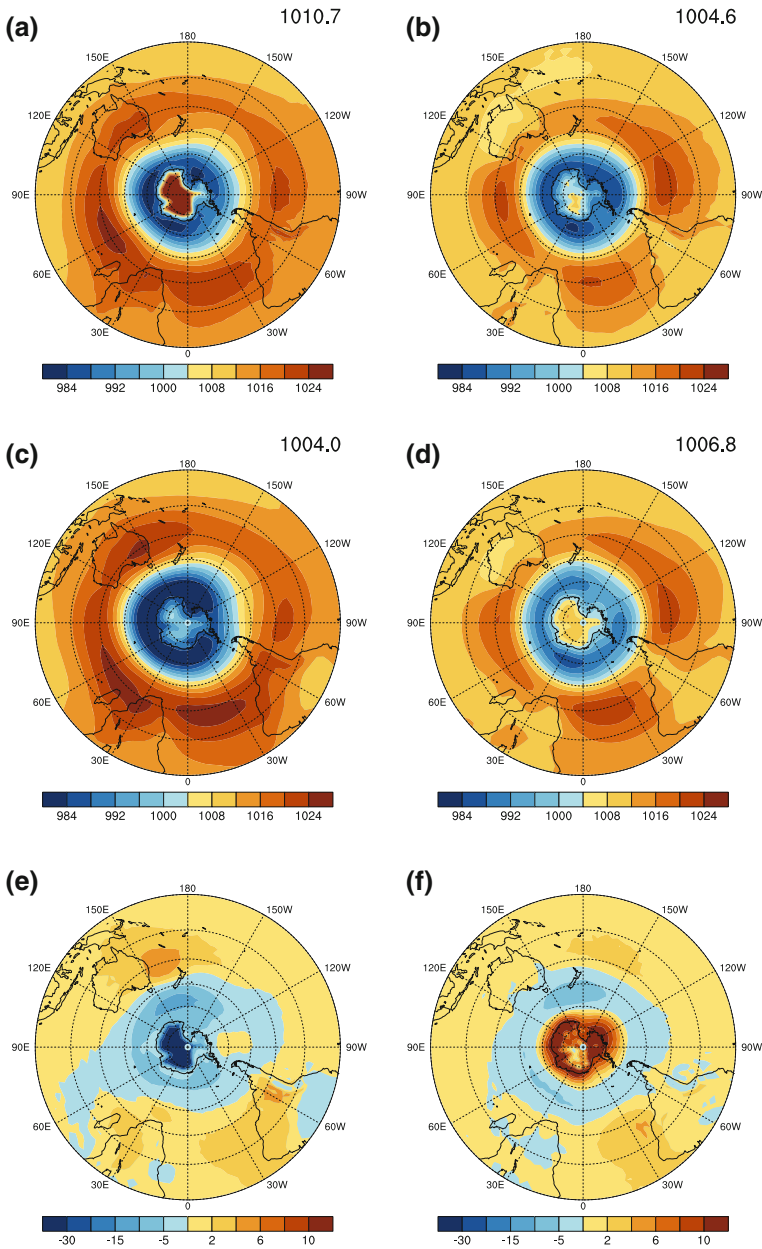


Fig. 19.1 June–July–August mean (*left row*) and December–January–February mean (*right row*) distributions of sea level pressure in the Southern Hemisphere from 1979 to 2005 (units: hPa): **a, b** national centers for atmospheric prediction data; **c, d** flexible global ocean–atmosphere–land system model, spectral version two, (FGOALS-s2) simulation; **e, f** difference between FGOALS-s2 and NCEP (after Zhou et al. 2013a)

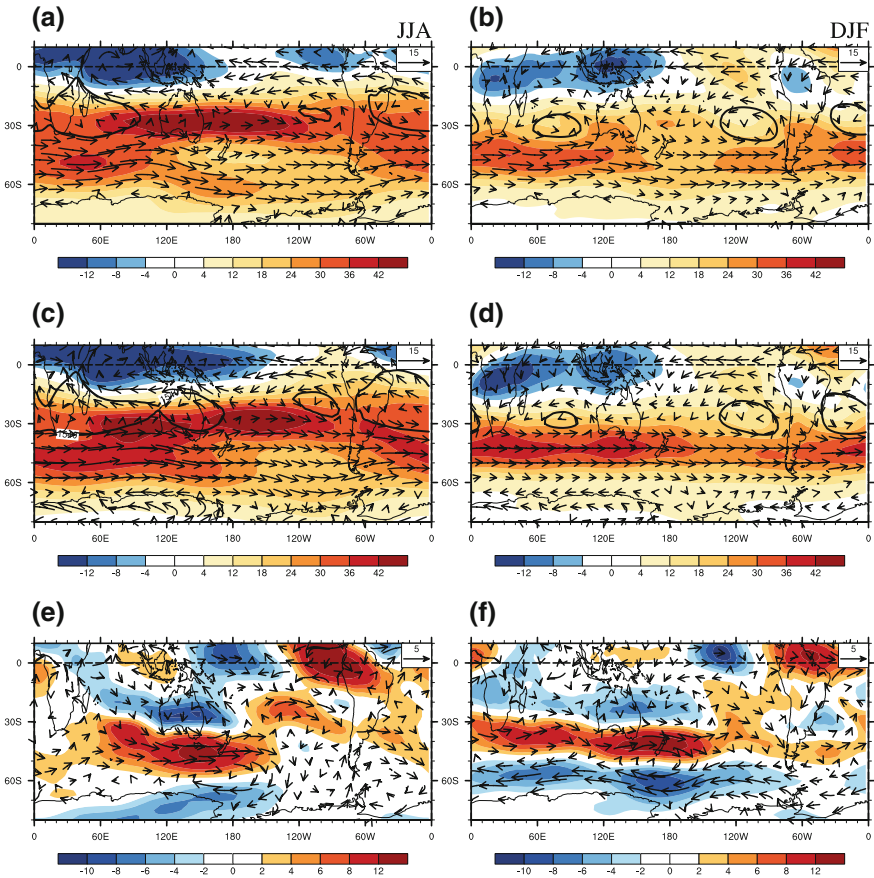


Fig. 19.2 Same as Fig. 19.1, but for the wind field at 850 hPa (vector, units: m/s) and zonal wind at 200 hPa (shaded, units: m/s). The *black thick line* represents the 1,540 gpm contour at 850 hPa geopotential height (after Zhou et al. 2013a)

19.3.2 Changes in MH, AH, and AAO Under Various RCPs

The changes in MH, AH, and AAO projected by FGOALS-s2 under various RCPs scenarios are shown in Fig. 19.3. Because the intensity of MH and AH are prominent in JJA, a 31-year running mean of the JJA MH and AH indices and their historical changes are given. In the observations, the intensity of MH was stronger than normal before the 1930s, weaker than normal between the 1930 and 1960s, and enhanced up to present stage. The observed interdecadal changes were partly reproduced by the model (Fig. 19.3a).

Under various RCPs scenarios, the MH index exhibited a weakening trend before the 2030s and a strengthening trend thereafter. During the period of

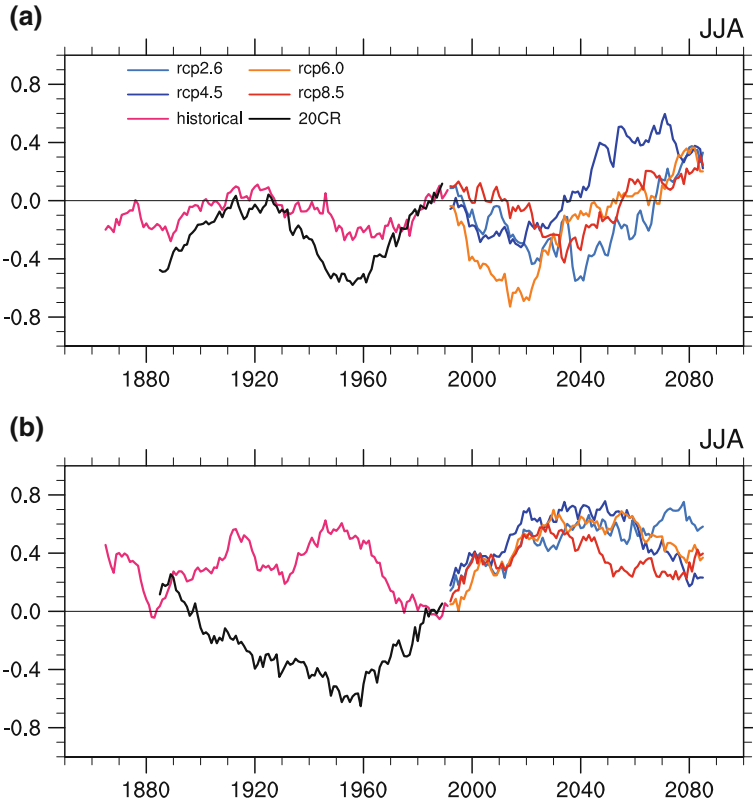


Fig. 19.3 The 31-year running mean of June–July–August mean **a** Mascarene High index and **b** Australian High index. The periods of the observation data are from 1870 to 2005; the history climate experiment data are from 1850 to 2005; and the RCPs scenario experimental data are from 2006 to 2100 (after Zhou et al. 2013a)

2006–2100, the index exhibited trends of 0.109, 0.102, 0.146, 0.054 hPa/10 yr under RCP scenarios 2.6, 4.5, 6.0, and 8.5 respectively.

The change in AH differed from that in MH; weakening was detected between the 1880 and the 1960s, after which time a recovery trend was evident. The model failed in reproducing this type of change. The projected changes in AH under the four RCPs scenarios were highly consistent and exhibited enhanced phases before the 2030s and a weakening trend afterward. Because MH is a subtropical high-pressure system and AH represents cold high pressure, the projected weakening trend of AH is expected.

Previous studies have indicated that both ozone and the greenhouse gases had significant impacts on the observed AAO trends in recent decades (Thompson and Solomon 2002; Gillett and Thompson 2003; Cai and Cown 2007). In the observation, the JJA AAO intensity enhancement began in the 1930s. In the model, however, same trend started in the 1960s (Fig. 19.4). Under RCP2.6 and RCP4.5

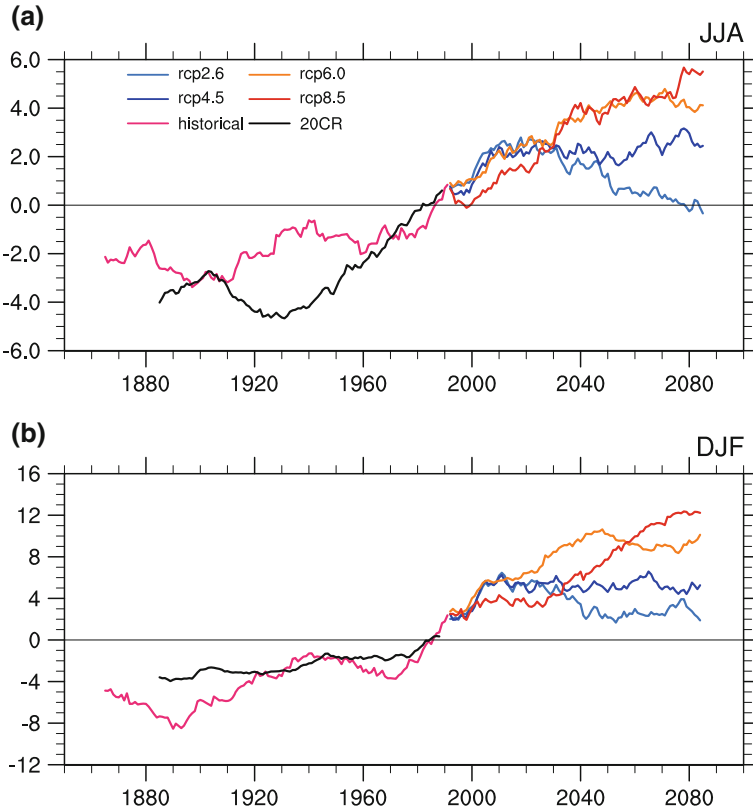


Fig. 19.4 Same as Fig. 19.3, but for **a** June–July–August mean Antarctic Oscillation index and **b** December–January–February mean AAO index (after Zhou et al. 2013a)

scenarios, AAO intensity exhibited a strengthening trend at the beginning of the twenty first century. However, under the RCP4.5 scenario the trend was not significant, and under the RCP2.6 scenario, the AAO also began a weakening trend in 2030s.

In DJF, the observed AAO trend showed a gradually increase from the 1880 to 2005s, which was partly reproduced in the simulation. The projected changes of AAO in DJF resembled that of JJA under RCP2.6 and RCP4.5 scenarios, such as an enhancing trend followed by a weakening trend. However, under the RCP6.0 scenario the AAO index exhibited an enhancing trend before the 2040s and was followed by a weakening trend. Under the RCP8.5 scenario the projected AAO change exhibited a significant strengthening trend.

In summary, under both RCP2.6 and RCP4.5 scenarios, the AAO initially intensified and later exhibited a weakening tendency, whereas under both RCP6.0 and RCP8.5 scenarios the AAO exhibited a significant strengthening trend. Previous studies also reported that once the CO_2 concentration stabilizes, the trend of

AAO reverses (Cai et al. 2003). In the RCP2.6 scenario, the total radiative forcing peaked at approximately 3 W/m^2 and declined thereafter; under the RCP4.5 scenario, the total radiative forcing stabilized after reaching 4.5 W/m^2 . The peak radiation forcings of RCP6.0 and RCP8.5 were 6.0 and 8.5 W/m^2 , respectively (Meinshausen et al. 2011). The changes in AAO are attributed to changes in radiation forcing under various scenarios.

19.4 Conclusion

The performance of IAP/LASG climate system model FGOALS-s2 in the simulation of the present-day climate in the Southern Hemisphere was assessed in the present study. Future changes in the Southern Hemispheric climate were projected for four RCPs scenarios. The major conclusions are summarized in this section.

Major features of climate mean states of the atmospheric circulation in the Southern Hemisphere were effectively simulated, including the reverse SLP anomaly distribution between subtropical and high latitudes and the double jet phenomenon in JJA, although the north (south) branch was weaker (stronger) than the observation.

Under the four RCPs scenarios, the intensity of the MH was weakened in the beginning of the twenty first century but was enhanced beginning in the 2030s, whereas the opposite was noted for AH. Although the future evolution of AAO is scenario-dependent, it showed clear intensification under RCP6.0 and RCP8.5 scenarios. Preliminary analysis showed that AAO changes under the various RCPs scenarios were dominated by various temperature changes in the vertical direction. For example, both RCP6.0 and RCP8.5 emission scenarios exhibited an enhanced meridional temperature gradient and thus an enhanced mid-latitude westerly jet favorable for a stronger AAO.

Acknowledgments This work was supported by the “Strategic Priority Research Program—Climate Change: Carbon Budget and Related Issues” of the Chinese Academy of Sciences (Grant No. XDA05110301).